Journal of Alloys and Compounds 586 (2014) S24–S30

Contents lists available at SciVerse ScienceDirect

Journal of Alloys and Compounds

journal homepage: www.elsevier.com/locate/jalcom

Air-oxidation of a $Pd_{40}Ni_{40}P_{20}$ bulk glassy alloy at 250–420 °C

W. Kai [a,*], Y.H. Wu [a], I.F. Jen [b], T.H. Ho [a], H.H. Hsieh [c]

[a] Institute of Materials Engineering, National Taiwan Ocean University, Keelung 20224, Taiwan, ROC
[b] United Microelectronics Corporation, Xinshi Dist., Tainan City 74147, Taiwan, ROC
[c] Institute of Technical Research Industries, Hsin-Chu 31005, Taiwan, ROC

ARTICLE INFO

Article history:
Available online 16 February 2013

Keywords:
Oxidation
$Pd_{40}Ni_{40}P_{20}$ bulk-metallic glass
NiO
Pd_3P
Ni_3P

ABSTRACT

The oxidation behavior of a $Pd_{40}Ni_{40}P_{20}$ bulk-metallic glass (Pd3-BMG) was studied over the temperature range of 250–420 °C in dry air. The Pd3-BMG revealed nearly no oxidation at $T < 300$ °C, while its oxidation kinetics followed a multiple-stage parabolic-rate law at $T \geqslant 300$ °C, with its oxidation rates increasing with temperature. In general, the oxidation rate constants (k_p values) of Pd3-BMG are slightly higher than those of the crystalline counterpart and polycrystalline pure Ni at 300–420 °C, indicating that the amorphous alloy exhibited a poor oxidation resistance. An exclusive layer of NiO scale formed on the alloy surface and a Pd-enriched layer was also observed beneath the scale. In addition, the amorphous substrate transferred into two crystalline phases of Pd_3P and Ni_3P after the oxidation at $T \geqslant 300$ °C, indicative of the occurrence of phase transformation.

1. Introduction

In the past decades, bulk metallic glasses (BMGs) have been widely studied for several possible applications because many developed BMG systems exhibited excellent strength, stiffness and better physical/chemical properties, as compared to commercial crystalline alloys [1–3]. In a review of the development of BMGs, the Pd-based glassy alloy containing Cu and Si additions was the first ternary BMG prepared by a simple suction-casting technique in 1974 [4]. Since then, a number of precious-metal-based glassy alloys, such as Pd- and Au-based BMGs were prepared [5–7]. It was generally found that most Pd-based BMGs not only exhibited better mechanical properties, but possessed excellent glass forming ability (GFA) and larger supercooled temperature (ΔT_x). For example, the $Pd_{40}Ni_{40}P_{20}$ bulk-metallic glass (Pd3-BMG) exhibited a high yielding strength of ~1600 MPa and a fracture strength of ~1700 MPa in room-temperature compression [8]. In addition, this glassy alloy had a larger ΔT_x value of ~72 °C, which offered a better welding ability and superplasticity (up to a 1260% deformation) [9]. Besides, it was reported that the quaternary version of this family, the $Pd_{43}Cu_{27}Ni_{10}P_{20}$ bulk-metallic glass (Pd4-BMG), could retain its amorphous structure in a relative lower critical cooling rate (~4 °C/min), as compared to that of the ternary alloy (~60 °C/min) [10]. The quaternary alloy systems exhibited interesting mechanical properties when certain amounts of porosity were present inside the materials (i.e., metallic glass foam) [11]. For example, in the porosity range of 36 to 70%, $Pd_{42.5}Cu_{30}Ni_{7.5}P_{20}$ and $Pd_{43}Cu_{27}Ni_{10}P_{20}$ foams exhibited strengths in the range of 6–32 MPa [12,13]. Furthermore, the oxidation behavior of both Pd4-BMG and its foam (PD4-AF) containing 45% porosity was previously investigated in our laboratory [14], and the results showed that no detectable oxidation was observed for both glassy alloys at $T < 250$ °C. The oxidation kinetics of the two alloys followed a two-stage parabolic-rate law from 250 to 350 °C, and the steady-state k_p values generally increased with temperature. Interestingly, an exclusive CuO layer formed on both alloys although the k_p values of the Pd4-BMG are slightly faster than those of the Pd4-AF, which resulted in a better oxidation resistance with respect to that of pure Cu which formed duplex scales of CuO/Cu_2O. However, the oxidation behavior of the Pd3-BMG has been neither studied nor reported in the literature. Thus, the goal of this work is to study air oxidation of Pd3-BMG, in particular, the role of alloying elements (Ni and P) on the scale formation and the crystallization of the amorphous substrate will be explored.

2. Experimental

The starting materials contained high purity of Pd and Ni turnings (both > 99.95% pure) as well as P nodules (>99.99%). The Pd3-BMG rod with 5.5 mm in diameter and 50.0 mm in length was prepared by an injection-casting technique [15]. The average composition of the amorphous alloy was determined by an X-ray wavelength-dispersive spectrometer (WDS) is 39.9% Pd, 40.6% Ni, and 19.5% P (hereinafter in atomic percent unless otherwise stated). The oxidation samples were directly sheared from the length of the amorphous rod to the disks (~1.5 mm thick), ground and polished down to 1200 SiC abrasive papers, cleaned with acetone, and immediately dried before the tests. For comparative purposes, the crystalline counterpart of the alloy (XPd3) was prepared by vacuum-annealed the sheared disks at 700 °C for 1 h. In addition, pure Ni sheets (99.95% pure) with

---

* Corresponding author. Tel.: +886 2 2462 2192 (#6403).
E-mail address: wkai@email.ntou.edu.tw (W. Kai).

0925-8388/$ - see front matter Crown Copyright © 2013 Published by Elsevier B.V. All rights reserved.
http://dx.doi.org/10.1016/j.jallcom.2013.01.175

their average grain size ~50 μm were also directly sheared into the rectangle-shaped samples (5 × 4.5 × 1.5 mm). Both pure Ni and XPd3 samples also followed the same grinding and polishing procedures described above.

The thermal stability of the Pd3-BMG was examined by differential scanning calorimetry (DSC) at various heating rates from 10 to 100 °C/min. Oxidation tests of pure Ni and the two alloys were carried out by means of a thermogravimetric analyzer (TGA) in dry air (>99.999 vol.% pure). The heating and cooling rates of TGA were set at 10 °C/min, and the net flow rate of air was kept constant at 40 cm^3/min throughout each test. The characterization of the alloys and scales was performed using X-ray diffraction (XRD), a scanning electron microscope (SEM) equipped with an energy-dispersive spectrometer (EDS), an electron probe microanalyzer (EPMA) equipped with a WDS, and a transmission electron microscope (TEM) equipped with an EDS, image analyzer, and selected-area diffraction (SAD).

3. Results and discussion

3.1. Substrate analyses

The XRD spectra of the as-cast Pd3-BMG and XPd3 are shown in Fig. 1, revealing that the amorphous alloy is characterized by a wide-broadening peak near $2\theta = 41.9°$, which further indicated the amorphous structure. On the other hand, two phase structure was observed for the XPd3 alloy, consisting of Ni_3P and Pd_3P. The DSC curves of the Pd3-BMG shown in Fig. 2 reveal that both the glass transition temperature (T_g) and the crystalline temperature (T_x) steadily increased with increasing heating rate. All the values of characteristic temperatures are summarized in Table 1. The typical T_g and T_x temperatures at a heating rate of 10 °C/min are 289.7 and 379.2 °C, respectively, and the supercooled liquid region ($\Delta T_x = T_x - T_g$) of the Pd3-BMG is about 89.5 °C, which is slightly higher than that reported in the literature [9]. Thus, the oxidation tests were set over from 200 to 420 °C to cover all the possible transaction regions.

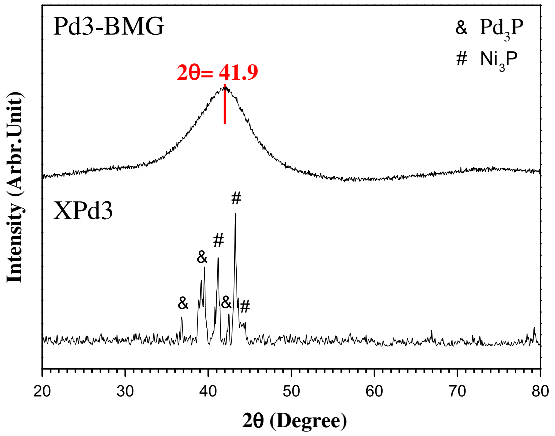

Fig. 1. XRD analyses of Pd3-BMG and XPd3.

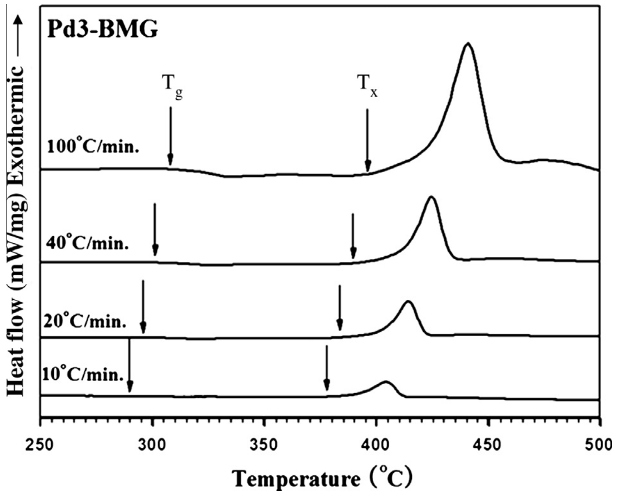

Fig. 2. DSC curves of Pd3-BMG at various heating rates.

3.2. Oxidation kinetics

Parabolic plots of the oxidation kinetics of the Pd3-BMG over the temperature range of 250–420 °C are shown in Fig. 3a. The oxidation kinetics of the glassy alloy was very complex and temperature-dependent. Generally speaking, a three-stage parabolic-rate law was obeyed for the ternary glassy alloy at 390 and 420 °C, consisting of a fast-growth transient oxidation (up to around 2.5 h), followed by a decreased second stage (from 2.5 to 4.5 h), and then, by a third steady-state stage of the intermediate rate (5–48 h). On the other hand, a two-stage parabolic-rate law was observed at lower temperatures (300–350 °C), consisting of a slow-growth stage (up to about 45 min) and a later steady-state stage. In addition, the steady-state k_p values were calculated by the square of the slope in the figure (dashed line) as an equation between the mass-gain data and the exposure duration of time (t):

$$(\Delta m/A)^2 = k_p t + C \tag{1}$$

where Δm, A, and C are the mass-gain data, specimen area, and integration constant, respectively. Nevertheless, the observed parabolic kinetics indicated that solid-state diffusion is the rate-determining step throughout the oxidation. Furthermore, the oxidation kinetics of the Pd3-BMG at 250 °C was nearly invisible, which was nearly parallel to the abscissa of the figure. However, the enlarged plot in Fig. 3b showed that the mass-gain datum at that temperature revealed significantly fluctuated feature, implying that the mass gain was very small, about 9.3×10^{-6} g/cm^2 after a 48-h exposure. Besides, although not shown here, attempts to oxidized two Pd3-BMG samples at 200 and 225 °C for 48 h were not successful because the overall mass-gain data were negligible and beyond the TGA detection limits.

For comparative purposes, the oxidation–kinetics curves of the crystalline counterpart over the temperature range of 300–420 °C are also shown as the parabolic plot in Fig. 3c. The oxidation kinetics also followed a multi-stage parabolic-rate law although larger data scattering was noted at all temperatures. The k_p values of polycrystalline pure Ni, Pd3-BMG, and XPd3 obtained in the same atmosphere are tabulated in Table 2 for comparison. Interestingly, the k_p values of the Pd3-BMG are slightly higher than those of pure Ni and the crystalline counterpart, indicating that the amorphous alloy exhibited a poor oxidation resistance at 300–420 °C. The observed discrepancy of the k_p values for Pd3-BMG with respect to XPd3 and pure Ni may deserve further microstructure study, as described below.

3.3. Scale constitution and phases

Typical cross-sectional backscattered-electron-image (BEI) micrographs of the scales of formed on the crystalline counterpart

Table 1
The values of thermal properties of Pd3-BMG at various heating rates.

	T_g (°C)	T_x (°C)	ΔT_x (°C)
10 °C/min	289.7	379.2	89.5
20 °C/min	294.5	382.1	87.6
40 °C/min	300.7	387.6	86.9
100 °C/min	308.7	397.9	89.2

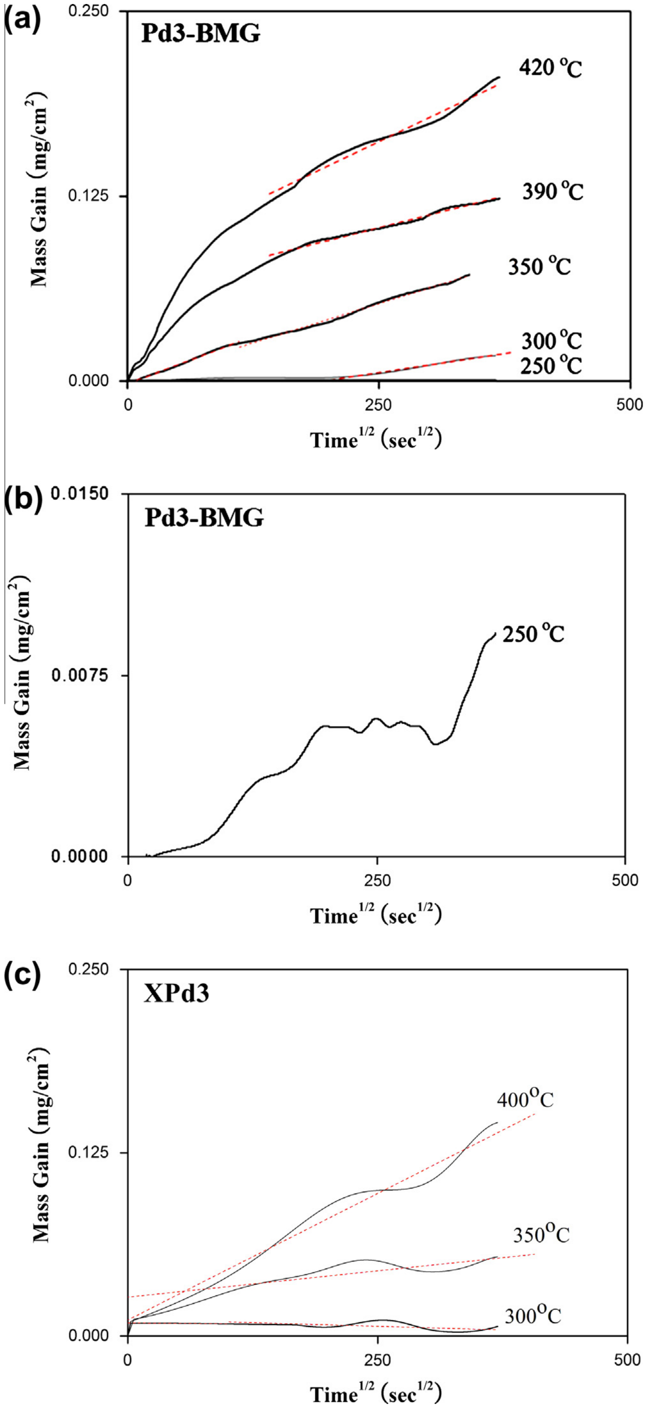

Fig. 3. Parabolic plots of oxidation kinetics at 250–420 °C for (a) Pd3-BMG and (b) the enlarged plot of (a), and (c) XPd3.

Table 2
The parabolic-rate constants of thePd3-BMG and pure Ni (g^2/cm^4/s).

	250 °C	300 °C	350 °C	390 °C	420 °C
Pure Ni	–	–	4.4×10^{-15}	–	3.9×10^{-14}
Pd3-BMG	–	4.7×10^{-15}	8.1×10^{-15}	2.9×10^{-14}	4.9×10^{-14}
XPd3	–	2.8×10^{-15}	3.8×10^{-15}	–	3.8×10^{-14}

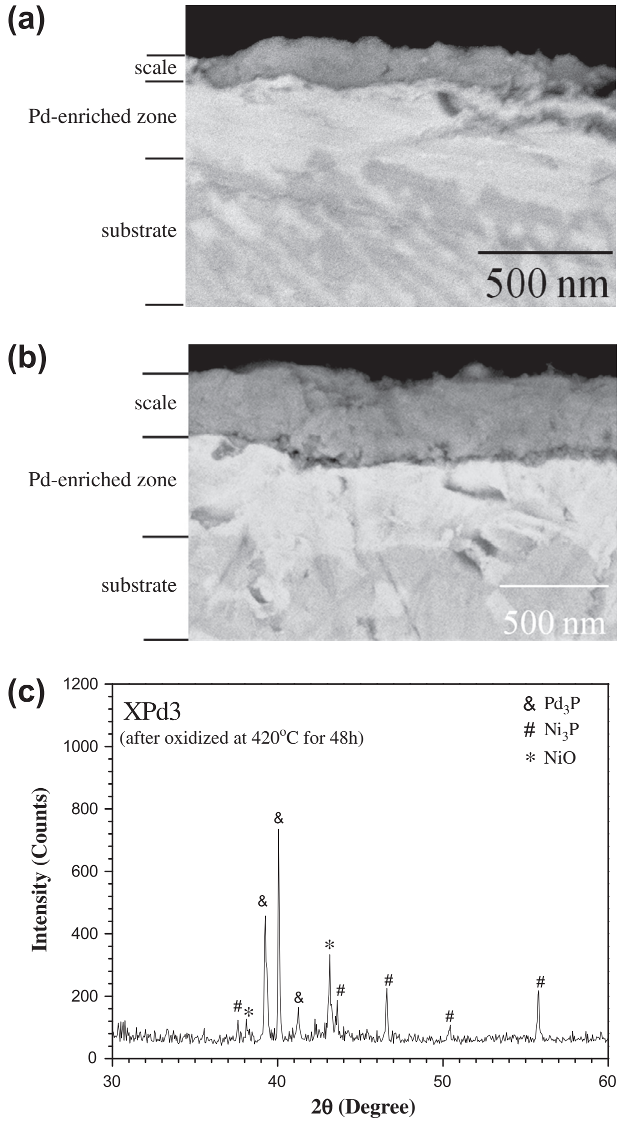

Fig. 4. Cross-sectional BEI micrographs of the scales from on XPd3 oxidized for 48 h at (a) 350 °C, (b) 420 °C, and (c) XRD spectra of (b).

(the XPd3 alloy) oxidized for 48 h at 350 and 420 °C are shown in Fig. 4a and b. A thin single-layer scale formed on the crystalline counterpart with an average thickness was about 149.6 ± 21.4 and 255.3 ± 47.9 nm at 350 and 420 °C, respectively. The observed thin-scale thickness is in good agreement with the slower kinetics for this crystalline alloy. XRD analyses (Fig. 4c) at 420 °C revealed that an exclusive NiO intermixed with Pd_3P and Ni_3P phases formed on the alloy. An important aspect to mention here is the presence of a bright zone beneath the NiO scale, whose thickness gradually increased with temperature, being around 330.4.6 ± 51.6 nm at 350 °C and 401.3 ± 65.5 nm at 420 °C. EDS analyses for four different regions gave the average composition of Pd (72.8%), P (24.7%), Ni (2.5%) and no O, which is close to the Pd_3P phase dissolved with minor Ni.

The surface topographies of Pd3-BMG after the oxidation at 250 °C for 48 h is shown in Fig. 5a, revealing only a few discontinuous, granular precipitates formed on the surface. Note that numerous striations of the sample after grinding with #1200 SiC abrasive papers still retained at most areas, which further indicated that the oxidation of the glassy alloy at this temperature was negligible. At higher magnification of the inserted photo, submicron-sized oxide clusters were observed. EDS analyses gave the average composition of high Ni (30.27%) and O (53.31%), but low Pd (12.08%) and P (4.35%), which may indicate to form the NiO

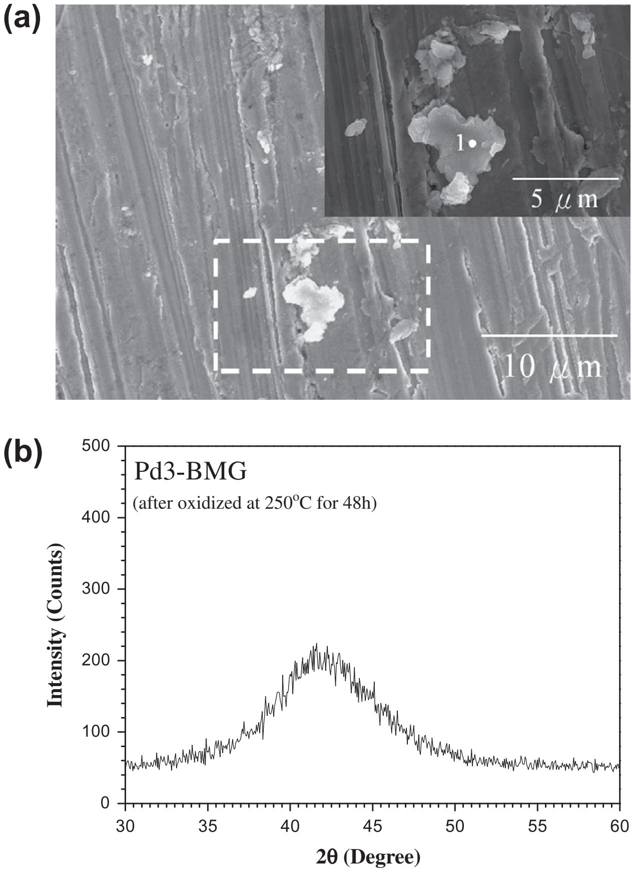

Fig. 5. Surface topography of Pd3-BMG after the oxidation for 48 h at (a) 250 °C and (b) corresponding XRD spectra of (a).

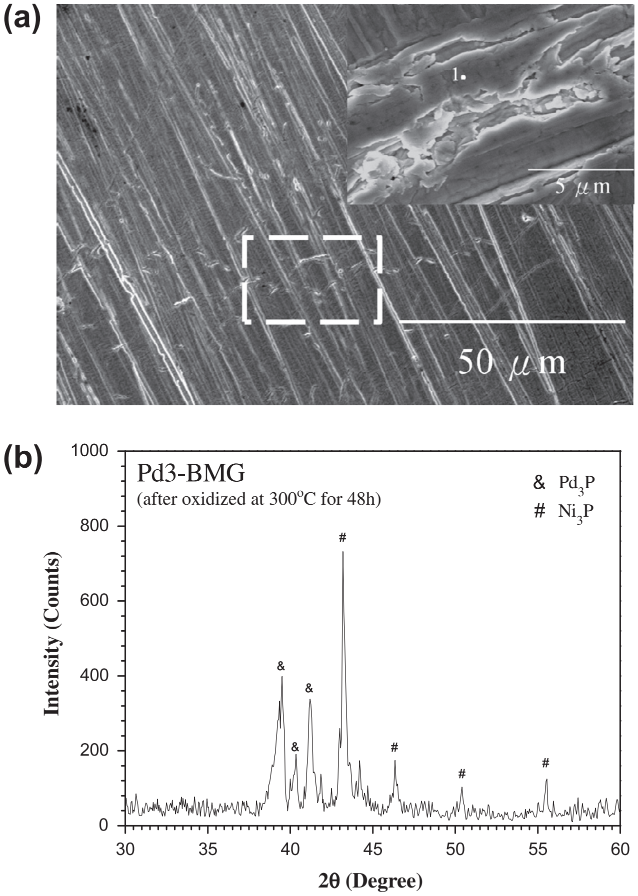

Fig. 6. Surface topography of Pd3-BMG after the oxidation for 48 h at (a) 300 °C and (b) corresponding XRD spectra of (a).

phase. Nevertheless, the amounts of oxide granules were not so abundant, which was in good agreement with a very-slow oxidation rate, as described above. In addition, XRD analyses of this oxidized sample shown in Fig. 5b only revealed a wide-broadening peak at $2\theta \sim 41.9°$. This observation further confirmed that the Pd3-BMG substrate remained amorphous nature even it was exposed for 48 h at this temperature. As similar to the formation of discontinuous oxide precipitates on the glassy alloy, Fig. 6a showed another Pd3-BMG sample oxidized at 300 °C for 48 h, in which the amounts of NiO were much abundant and the size of the clusters was much larger than that at 250 °C. XRD analyses in Fig. 6b only revealed two crystalline phases of Pd_3P and Ni_3P, while the NiO phase was completely absent. This may be due to its lower amounts below the X-ray detection limits. Nevertheless, the observed two crystalline phases further indicated that the amorphous substrate started to crystallize at this temperature after a 48-h exposure. As recalled previously [14], the Pd4-BMG substrate transformed into three crystalline phases of Pd_3P, Cu_3P, and Pd_2Ni_2P after the oxidation at 250–350 °C for 48 h, one may expect a similar phase transformation to form Pd_3P and Pd_2Ni_2P (but no Cu_3P) in the ternary glassy amorphous. However, the results obtained above indicated that Ni_2P instead of Pd_2Ni_2P formed on the substrate. The reason for this discrepancy is still unclear, and remains an unsolved puzzle in the current study.

Unlike the formation of discontinuous granular oxide-precipitates at 300 °C or lower, a thin layer-scale was always present for the glassy alloy exposed for 48 h at higher temperatures ($T \geqslant 350$ °C), as shown by the cross-sectional BEI micrographs at various temperatures in Fig. 7. A uniform oxide-layer formed on top of the glassy alloy remained good adherence to the substrate, and the thickness of the scale was around 185.6 ± 28.2, 225.8 ± 23.1, and 374.7 ± 68.1 nm at 350, 390, and 420 °C, respectively. In other words, the thickness of the scale steadily increased with temperature, implying that the higher the temperature, the thicker the scale layer and the faster the oxidation rate. Thus, the observed scale-thickness change is also in good agreement with the kinetics measurements. Furthermore, it was also found that the scale thickness formed on the glassy alloy is slightly thicker than that grew at the XPd3 alloy, which further confirmed the faster oxidation rates for the Pd3-BMG alloy although an exclusive layer of NiO was observed on both alloys. Besides, the substrate just beneath the NiO scale also revealed a bright zone, which may be a Pd_3P precipitate region as similar to that of XPd3. However, its thickness (around 119.9 ± 33.9 and 348.2 ± 67.7 nm at 350 and 420 °C, respectively) is slightly thinner with respect to that in the crystalline alloy mentioned above.

An interesting aspect to discuss here is the formation of an exclusive NiO layer since no evidence of other oxides was detected by XRD and EDS. According to thermodynamic data [16], the Gibbs free energy of formation (ΔG_f° in the same unit of KJ/mol O_2) of P_2O_5 was around −481.3 at 350 °C, which was much negative than those of NiO (−363.9) and PdO (−102.7). In addition, although not shown here, other temperatures indeed followed a similar trend as that at 350 °C. Thus, the less negative value of Gibbs free energy for PdO may indicate that Pd can be considered relatively inert with respect to Ni and P, so that its reaction with oxygen to form PdO could be kinetically unfavorable. On the other hand, the formation of P_2O_5 should be thermodynamically favorable because the dissociation partial pressures of oxygen were much lower than the local

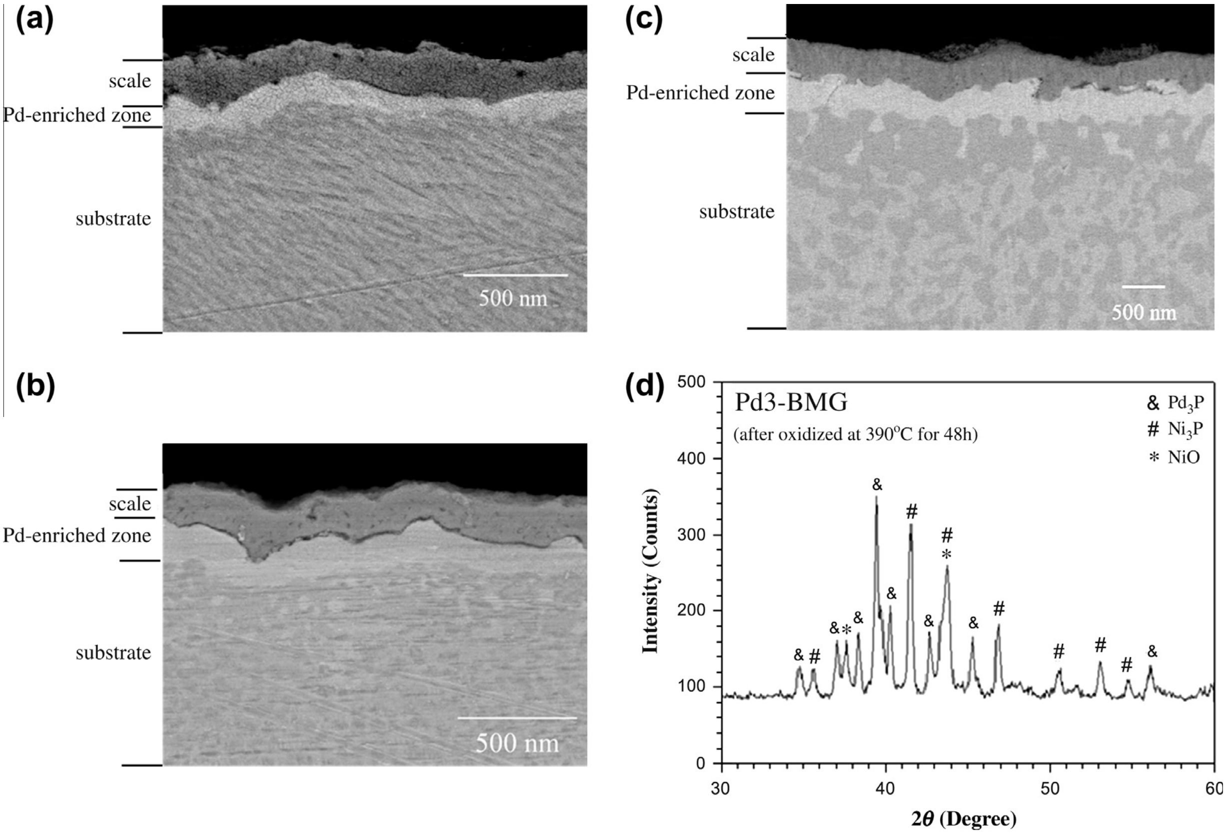

Fig. 7. Cross-sectional BEI micrographs Pd3-BMG after oxidation for 48 h at (a) 350 °C (b) 390 °C (c) 420 °C and the corresponding XRD spectra of (b).

oxygen partial pressure between nickel oxide and the substrate. However, XRD and EDS results described above confirmed its absence over the temperature range of study, which can be further ascribed to two possible reasons. The first reason is due probably to a faster scaling rate of NiO than that of P_2O_5, which may consume certain amounts of oxygen and nickel, and in turn, locally reduce the oxygen activity but increase the concentrations of Pd and P in the scale/substrate boundary. Since both atoms did not involve any oxidation, it could be possible that they can either retain in the scale or diffuse back into the substrate. The fact is that the microstructure analyses confirmed the growth of the Pd-enriched Pd_3P zone at the position beneath the NiO scale, which further indicated that the latter case should be more favorable in the current study. As a result, the formation of the Pd_3P zone to replace the oxidation of Pd and P become kinetically favorable. The second reason is due certainly to a higher activity of Ni than that of P, which gave nickel a better probability to react with oxygen to form NiO that intermixed with Pd_3P and Ni_3P in the scale of Pd3-BMG.

Furthermore, one would expect that an uncertain, analyzed error may take place because the spot size of EDS (1–2 μm) is much larger than the thickness of both NiO and the Pd-enriched zone (<1 μm). This situation deserves the further characterization of the exact constitution and phase identification of the oxidized sample through TEM analyses. A typical TEM bright-field image of the cross-section taken from the bright zone just beneath the scale formed on Pd3-BMG after the oxidation at 350 °C for 48 h was prepared; the results together with the corresponding SAD patterns were shown in Fig. 8a. The elongated white precipitate with about 900 nm in length and 250 nm in width was observed, and its SAD results with an aperture size of 20 μm came out in spot patterns under the zone axis of [1 −2 1] for the Pd_3P phase. Thus, TEM analyses confirmed the presence of Pd_3P in the bright zone of the substrate just beneath the scale. In addition, typical cross-sectional TEM bright-field micrographs taken from another Pd3-BMG sample at various regions after the oxidation at 390 °C for 48 h were further shown in Fig. 8b and c. A smaller white precipitate (around 300 nm in length and 150 nm in width) inside the substrate was observed, and its SAD spot-patterns were verified to be the Ni_3P phase under the zone axis of [−1 3 1], as shown in Fig. 8b. On the other hand, a thin layer-scale formed on the surface was observed, and the SAD spot-patterns taken from a dark granule within the white circle in the figure confirmed the existence of NiO. Thus, it may conclude that both Pd3-BMG and its crystalline counterpart experienced their oxidation by forming an exclusive NiO scale.

Another interesting aspect to further discuss is the possible reasons for the discrepancy of the oxidation rates for Pd3-BMG with respect to its crystalline alloy and pure Ni. Since all the materials oxidized to form the NiO scale, the observed faster oxidation rate for the amorphous alloy is due presumably to the presence of the excess free volume, as suggested in previous literature [17,18]. In other words, an amorphous alloy normally contains certain amounts of free volume inside its ingot after the solidification from liquids. It is very likely that a small amount of free volume provides a short circuit path for fast outward diffusion of Ni, which in turn enhances the oxidation reaction of the Pd3-BMG with respect to pure Ni although both samples formed a similar NiO layer after the oxidation.

3.4. Short-term oxidation

To understand the oxidation and crystallization behavior of the Pd3-BMG, short-term oxidation tests were carried at 300, 350, and 390 °C for various durations of time. A typical result of the XRD analyses of this alloy oxidized at 350 °C is shown in Fig. 9. Clearly, small amounts of Pd_3P and Ni_3P were formed on the amorphous

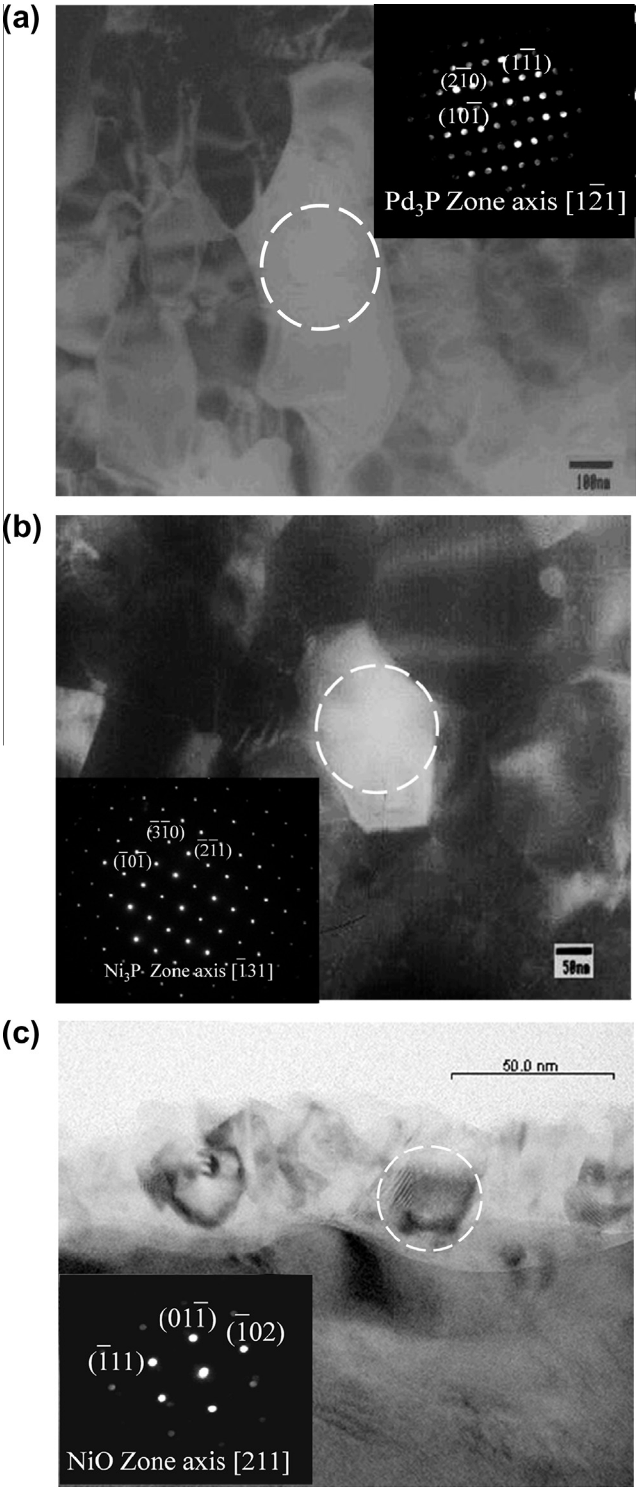

Fig. 8. TEM bright-field micrographs and inserted SAD patterns of Pd3-BMG oxidation at for 48 h (a) at 350 °C, (b) and (C) at 390 °C.

substrate after an initial oxidation for 7 min although the background of the wide-broadening peak was still present. In addition, the wide-broadening background was completely missing after a 20-minute exposure, while minor amounts of NiO were observed after a prolonged oxidation for 300 min (5 h). Thus, the whole phase transformation of the Pd3-BMG alloy after exposure in dry air was governed by the first crystallization of Pd_3P and Ni_3P, and then, the formation of NiO at the later stage of oxidation.

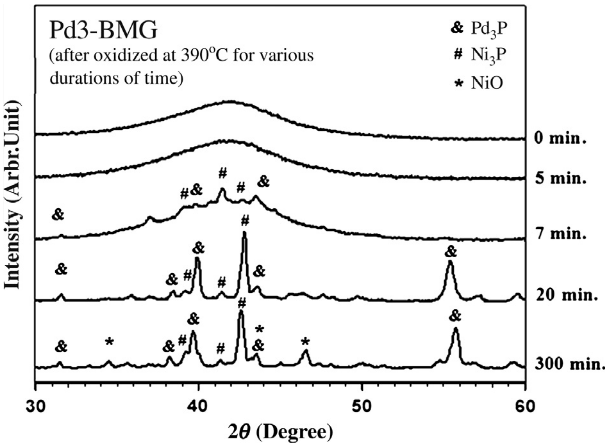

Fig. 9. XRD analyses of Pd3-BMG exposed at 350 °C for various duration of time.

4. Conclusions

The oxidation behavior of a $Pd_{40}Ni_{40}P_{20}$ bulk-metallic glass (Pd3-BMG) and its crystalline counterpart over the temperature range from 250 to 420 °C in dry air has been characterized. Several conclusions were drawn.

1. The oxidation kinetics of the amorphous alloy and its crystalline counterpart followed a multi-stage parabolic-rate law at 300–420 °C, while no detectable oxidation was observed at 250 °C or lower temperatures.
2. The oxidation rate constants of Pd3-BMG were slightly higher than those for pure Ni and the crystalline alloy, indicative of a poor oxidation resistance for the glassy alloy.
3. The scale formed on all tested materials, consisting of pure Ni, the amorphous and crystalline alloys consisted of an exclusive NiO layer.
4. The amorphous substrate started to transfer into two crystalline phases of Pd_3P and Ni_3P after the oxidation at 300 °C or higher, indicating that a phase transformation was taken place.

Acknowledgments

The authors are greatly thankful the partly financial support by the National Science Council of the Republic of China under Grant Nos. NSC 96-2218-E-011-001 and NSC 100-2221-E-019-032. The SEM and TGA equipment supports from the National Taiwan Ocean University under Grant Nos. of NTOU-AF94-04-03-01-01 and NTOU-RD972-04-03-01-01 are acknowledged. The TEM technical assistance from Mr. C.T. Wu in the Department of System Engineering and Science, National Tsing Hua University (Hsin-Chu, Taiwan) is greatly appreciated. Special Thanks are due to Profs. Y. Kawamura in Department of Mechanical Engineering and Materials, Kumamoto University, Japan and T.G. Nieh in Department of Materials Science and Engineering, University of Tennessee, Knoxville, USA for their kindly supports on sample preparation.

References

[1] A. Inoue, High strength bulk amorphous alloys with low critical cooling rates (overview), Mater. Trans., JIM 36 (1995) 866–875.
[2] A. Inoue, Stabilization of metallic supercooled liquid and bulk amorphous alloys, Acta Mater. 48 (2000) 279–306.
[3] A. Inoue, Bulk amorphous and nanocrystalline alloys with high functional properties, Mater. Sci. Eng. A 304 (2001) 1–10.
[4] H.S. Chen, Thermodynamic considerations on the formation and stability of metallic glasses, Acta Metall. 22 (1974) 1505–1511.

[5] N. Nishiyama, A. Inoue, Glass-forming ability of $Pd_{42.5}Cu_{30}Ni_{7.5}P_{20}$ alloy with a low critical cooling rate of 0.067 K/s, Appl. Phys. Lett. 80 (2002) 568–570.

[6] N. Chen, D.V. Louzguine-Luzgin, G.Q. Xie, T. Wada, A. Inoue, Influence of minor Si addition on the glass-forming ability and mechanical properties of $Pd_{40}Ni_{40}P_{20}$ alloy, Acta Mater. 57 (2009) 2775–2780.

[7] J. Schroers, B. Lohwongwatana, W.L. Johnson, A. Peker, Gold based bulk metallic glass, Appl. Phys. Lett. 87 (2005). 061912–061912-3.

[8] T. Mukai, T.G. Nieh, Y. Kawamurac, A. Inoue, K. Higashi, Dynamic response of a $Pd_{40}Ni_{40}P_{20}$ bulk metallic glass in tension, Scripta Mater. 46 (2002) 43–47.

[9] Y. Kawamura, T. Nakamura, A. Inoue, Superplasticity in $Pd_{40}Ni_{40}P_{20}$ metallic glass, Scripta Mater. 39 (1998) 301–306.

[10] N. Nishiyama, A. Inoue, Stability and nucleation behavior of glass-forming Pd–Cu–Ni–P alloy with a critical cooling rate of 0.067 K/s, Intermetallics 10 (2002) 1141–1147.

[11] T. Wada, A. Inoue, Formation of porous Pd-based bulk glassy alloys by a high hydrogen pressure melting-water quenching method and their mechanical properties, Mater. Trans. 45 (2004) 2761–2765.

[12] T. Wada, K. Kawamura, N. Nishiyama, A. Inoue, Formation and mechanical properties of porous Pd–Pt–Cu–P bulk glassy alloys, Mater. Trans. 46 (2005) 2777–2780.

[13] M.D. Demetriou, J.C. Hanan, C. Veazey, M.D. Michiel, N. Lenoir, E. Ustundag, W.L. Johnson, Yielding of metallic glass foam by percolation of an elastic buckling instability, Adv. Mater. 19 (2007) 1957–1962.

[14] W. Kai, I.F. Ren, B. Barnard, P.K. Liaw, M.D. Demetriou, W.L. Johnson, Oxidation behavior of a $Pd_{43}Cu_{27}Ni_{10}P_{20}$ bulk metallic glass and foam in dry air, Metall. Mater. Trans. A 41A (2010) 1720–1725.

[15] T. Mukai, T.G. Nieh, Y. Kawamura, A. Inoue, K. Higashi, Effect of strain rate on compressive behavior of a $Pd_{40}Ni_{40}P_{20}$ bulk metallic glass, Intermetallics 10 (2002) 1071–1077.

[16] I. Barin, Thermodynamic Data for Pure Substance, third ed., VCH, Weinheim, Germany, 1995.

[17] Z.P. Lu, C.T. Liu, Glass formation criterion for various glass-forming systems, Phys. Rev. Lett. 91 (2003). 115505–115505-4.

[18] W. Kai, H.H. Hsieh, T.H. Ho, R.T. Huang, Y.L. Lin, Air-oxidation behavior of a $Cu_{60}Hf_{25}Ti_{15}$ bulk metallic glass at 375–520 °C, Oxid. Met. 68 (2007) 177–192.